HEPATOLOGY

HEPATOLOGY, VOL. 68, NO. 4, 2018

Lipotoxicity Induces Hepatic Protein Inclusions Through TANK Binding Kinase 1–Mediated p62/Sequestosome 1 Phosphorylation

Chun-Seok Cho,[1*] Hwan-Woo Park,[1,2*] Allison Ho,[1] Ian A. Semple,[1] Boyoung Kim,[1] Insook Jang,[1] Haeli Park,[1] Shannon Reilly,[1,3,4] Alan R. Saltiel,[1,3,4] and Jun Hee Lee[1]

Obesity commonly leads to hepatic steatosis, which often provokes lipotoxic injuries to hepatocytes that cause nonalcoholic steatohepatitis (NASH). NASH, in turn, is associated with the accumulation of insoluble protein aggregates that are composed of ubiquitinated proteins and ubiquitin adaptor p62/sequestosome 1 (SQSTM1). Formation of p62 inclusions in hepatocytes is the critical marker that distinguishes simple fatty liver from NASH and predicts a poor prognostic outcome for subsequent liver carcinogenesis. However, the molecular mechanism by which lipotoxicity induces protein aggregation is currently unknown. Here, we show that, upon saturated fatty acid-induced lipotoxicity, TANK binding kinase 1 (TBK1) is activated and phosphorylates p62. TBK1-mediated p62 phosphorylation is important for lipotoxicity-induced aggregation of ubiquitinated proteins and formation of large protein inclusions in hepatocytes. In addition, cyclic GMP-AMP synthase (cGAS) and stimulator of interferon genes (STING), upstream regulators of TBK1, are involved in lipotoxic activation of TBK1 and subsequent p62 phosphorylation in hepatocytes. Furthermore, TBK1 inhibition prevented formation of ubiquitin-p62 aggregates not only in cultured hepatocytes, but also in mouse models of obesity and NASH. *Conclusion:* These results suggest that lipotoxic activation of TBK1 and subsequent p62 phosphorylation are critical steps in the NASH pathology of protein inclusion accumulation in hepatocytes. This mechanism can provide an explanation for how hypernutrition and obesity promote the development of severe liver pathologies, such as steatohepatitis and liver cancer, by facilitating the formation of p62 inclusions. (Hepatology 2018; 68:1331-1346).

Incidence of obesity and its corresponding complications are increasing at an alarming rate.[(1)] Nonalcoholic fatty liver disease (NAFLD) is among many abnormalities associated with obesity and, in many patients, progresses to nonalcoholic steatohepatitis (NASH).[(2)] Although the precise molecular events involved in the development of NASH remain uncertain, it has been proposed that obesity-induced

Abbreviations: Baf, bafilomycin A1; BSA, bovine serum albumin; CD, choline-deficient; cGAS, cyclic GMP-AMP synthase; CK2, casein kinase 2; COL, collagen; CS, choline-sufficient; CTGF, connective tissue growth factor; DHA, docosahexaenoic acid; DHE, dihydroethidium; ER, endoplasmic reticulum; HCC, hepatocellular carcinoma; HFD, high-fat diet; IL, interleukin; KRTs, keratins; LAMP1, lysosome-associated membrane protein 1; LC3, microtubule-associated protein light chain 3; LFD, low-fat diet; LOX, lysyl oxidase; MMPs, matrix metalloproteinases; NAFLD, nonalcoholic fatty liver disease; NASH, nonalcoholic steatohepatitis; Nrf2, nuclear factor erythroid 2-related factor 2; OA, oleic acid; PA, palmitic acid; PECAM-1, platelet endothelial cell adhesion molecule 1; p-p62, phosphorylated p62; p-TBK1, phosphorylated TBK1; ROS, reactive oxygen species; SA, stearic acid; SDS, sodium dodecyl sulfate; SFAs, saturated fatty acids; shRNA, short hairpin RNA; α-SMA, α-smooth muscle actin; SQSTM1, sequestosome 1; STING, stimulator of interferon genes; TBK1, TANK binding kinase 1; Tg, thapsigargin; TIMPs, tissue inhibitors of metalloproteinase; UFAs, unsaturated fatty acids; WT, wild-type.

Received August 3, 2017; accepted December 12, 2017.

Additional Supporting Information may be found at onlinelibrary.wiley.com/doi/10.1002/hep.29742/suppinfo.

Supported by the NIH (R01DK102850 [to J.H.L.], T32GM008322 and T32AG000114 [to A.H.], R01DK060591 [to A.R.S.], and P30AG024824, P30DK034933, P30DK089503, and P30CA046592) and Korean NRF grants (2015R1A5A1009701 and 2015R1C1A1A01054654 [to H.W.P.]).

**These authors contributed equally to this work.*

View this article online at wileyonlinelibrary.com.

DOI 10.1002/hep.29742

Potential conflict of interest: Nothing to report.

elevation in plasma free fatty acid levels provokes lipotoxic injuries to cells in the liver.[2] Saturated fatty acids (SFAs) are major perpetrators of lipotoxic injuries to cells, whereas unsaturated fatty acids (UFAs) often confer protection against SFA-induced lipotoxicity. NASH is characterized by various consequences of lipotoxic injury to liver cells, such as hepatocyte ballooning, protein inclusion formation, ectopic cell death, inflammation, and fibrosis.[3-5] Obesity and NASH are also established risk factors for hepatocellular carcinoma (HCC).[6]

Formation of insoluble protein inclusions in hepatocytes is characteristic of a damaged liver for both mice and humans.[3-5,7-9] These inclusions are also the critical marker that distinguishes simple NAFLD from NASH[7,9] and consist primarily of ubiquitinated proteins such as keratins (KRT8/18) and the ubiquitin adaptor, p62/sequestosome 1 (SQSTM1).[3,8] Hepatic protein inclusions are closely linked to lipotoxic injuries and metabolic pathologies because they are frequently associated with fat droplet accumulation.[7] The mouse model of NASH, associated with large protein inclusions, is established by inducing obesity with a high-fat diet (HFD) and administering additional insults that provoke inflammation, such as choline deficiency,[10,11] transgenic gene modulation,[5,12] or hepatotoxin administration.[5] However, HFD-induced obesity per se is also sufficient to induce protein aggregates of ubiquitinated proteins and p62 that are insoluble in nonionic detergents.[13-15] Although these findings suggest a causal link between obesity and hepatic protein aggregates, we currently have a very limited understanding of how obesity-associated lipotoxicity promotes the formation of insoluble protein inclusions. Acquiring this understanding is important, especially because p62 accumulation in hepatocytes was recently demonstrated to facilitate obesity-associated liver fibrosis and HCC development.[12,16]

To investigate the mechanism of how protein aggregates are formed in NASH, we established an *in vitro* model in which SFAs, such as palmitic acid (PA) and stearic acid (SA), prominently induce insoluble inclusion bodies consisting of ubiquitinated proteins and p62 in the cytoplasm of human hepatoma HepG2 cells.[15] Using this system, as well as *in vivo* mouse models, we showed that attenuation of autophagic flux is one of the major causes of protein aggregate formation. In hepatocytes, obesity and SFA-induced lipotoxicity induce a prolonged elevation in cytosolic calcium, which interferes with the fusion between autophagosomes and lysosomes.[15] Interestingly, several stress signaling pathways, such as endoplasmic reticulum (ER) stress, oxidative stress, c-Jun N-terminal kinase, and p53 pathways, were not significantly involved in this protein inclusion process.[15]

Although autophagy inhibition may explain how protein inclusions can be formed upon lipotoxic injury, we observed that protein aggregates induced by simple autophagy inhibition were morphologically distinct from SFA- or obesity-induced protein inclusions. This histomorphological discrepancy suggests that additional unknown pathways may mediate the formation of hepatic protein inclusions. Here, using both cultured cells and animal models of lipotoxicity and obesity, we show that a signaling pathway leading to TANK binding kinase 1; TBK1 activation induces phosphorylation and aggregation of p62, which facilitates the lipotoxicity-induced formation of ubiquitinated protein inclusions. Because inhibition of the TBK1 pathway effectively and specifically attenuates ubiquitin-p62 protein inclusions and fibrotic liver pathologies, this pathway could be a promising target for the treatment of NASH or other diseases associated with autophagy defects and proteinopathy.

ARTICLE INFORMATION:

From the [1]Department of Molecular and Integrative Physiology, University of Michigan, Ann Arbor, MI; [2]Department of Cell Biology, Myunggok Medical Research Institute, Konyang University College of Medicine, Daejeon, Republic of Korea; [3]Life Sciences Institute, University of Michigan, Ann Arbor, MI; [4]Institute for Diabetes and Metabolic Health, Departments of Medicine and Pharmacology, University of California, San Diego, La Jolla, CA.

ADDRESS CORRESPONDENCE AND REPRINT REQUESTS TO:

Jun Hee Lee, Ph.D.
Department of Molecular and Integrative Physiology,
University of Michigan
109 Zina Pitcher Place
Ann Arbor, MI 48109-2200
E-mail: leeju@umich.edu
Tel: +1-734-764-6789

Materials and Methods

CELL CULTURE STUDIES

HepG2 cells were obtained from ATCC (HB-8065). Primary hepatocytes were isolated and cultured as described.[17] To induce lipotoxicity, de-lipidated low-endotoxin bovine serum albumin (BSA) was loaded with PA and other fatty acids, as described,[15,17] and applied to cultured cells. Details in cell-culture procedures are described in the Supporting Information.

ANIMAL STUDIES

Mice of C57BL/6 genetic background were used for this study. All animal studies were ethically approved and overseen by the University Committee on Use and Care of Animals at the University of Michigan (Ann Arbor, MI). Details in animal procedures, including mouse genotypes and their sources, number, age and sex of mice, diet treatment, and drug administration, are described in the Supporting Information and corresponding figure legends.

QUANTIFICATION AND STATISTICAL ANALYSIS

Immunoblotting images were quantified by densitometry, and protein expressions are expressed as relative band intensities. Colocalization of different proteins was expressed as line-scan evaluation graph or Pearson's coefficient. All the statistical analyses were performed with more than three independent biological replicates ($n \geq 3$) for cell-culture studies or with the indicated numbers of animals for *in vivo* mouse studies. Statistical significance of differences between two groups was calculated using a Student *t* test ($^{*}P < 0.05$; $^{**}P < 0.01$; $^{***}P < 0.001$).

OTHER METHODS

For details of reagents, lentiviral constructs, subcellular fractionation, protein analysis, immunocytochemistry, and histology, see the Supporting Information.

Results

SFA INDUCES LARGE p62/SQSTM1 INCLUSIONS WHILE OTHER AUTOPHAGY INHIBITORS DO NOT

We and others have formerly shown that thapsigargin (Tg), bafilomycin A1 (Baf), and SFA interfere with autophagic flux, mainly through elevation of cytosolic calcium and subsequent inhibition of autophagosomal-lysosomal fusion.[15,18,19] However, we noticed that the patterns of p62 inclusions formed from SFA-induced lipotoxicity are apparently distinct from what we observed in Tg- and Baf-treated human hepatoma HepG2 cells. PA-induced protein aggregates appear as rod-shaped sizable inclusions in the cytoplasm (Fig. 1A), similar to hepatic protein inclusions observed during NASH[4] and NASH-associated HCC,[12] whereas Tg- or Baf-induced p62 aggregates are observed as numerous small puncta (Fig. 1A). This obvious difference suggests that, in addition to modulating the calcium signaling, lipotoxic insults modulate unknown target(s) that control the morphology of the p62-ubiquitin inclusion bodies.

The protein inclusions found in NASH are called Mallory-Denk bodies, which consist mainly of ubiquitinated KRT8/18 and p62.[3,8] Although we knew that the SFA-induced protein aggregates in HepG2 cells are enriched with p62 and ubiquitinated proteins (Fig. 1A-D),[20] we wanted to identify which specific proteins are found in this protein inclusion. Therefore, we isolated insoluble protein fractions from control and PA-treated cells, and subjected them to sodium dodecyl sulfate (SDS)/polyacrylamide gel electrophoresis and Coomassie staining (Supporting Fig. S1A). Then, we searched for protein bands that were specifically enriched in PA-treated cells. From this analysis, we identified a ~54-kDa band as one of the most prominently enriched bands in the insoluble fraction from the PA-treated cells (Supporting Fig. S1A). Tandem mass spectrometry analysis revealed that this band corresponds to KRT8 (Supporting Fig. S1A), supporting the close relationship between our PA-induced protein inclusions and the Mallory-Denk bodies. Therefore, this SFA-induced lipotoxicity model provides a pathophysiologically relevant experimental system for modeling NASH-associated protein inclusions.

SFA INDUCES PHOSPHORYLATION OF p62 AT SERINE 403

p62 proteins accumulated under SFA-induced lipotoxicity exhibited strong electrophoretic mobility retardation (band shift; Fig. 1B), suggesting posttranslational modification of the protein. Although the calcium-channel blocker, verapamil, strongly suppressed p62 accumulation by restoring autophagic flux,[15] it did not inhibit the p62 band shift (Fig. 1B), suggesting that this modification is not controlled by calcium-autophagy

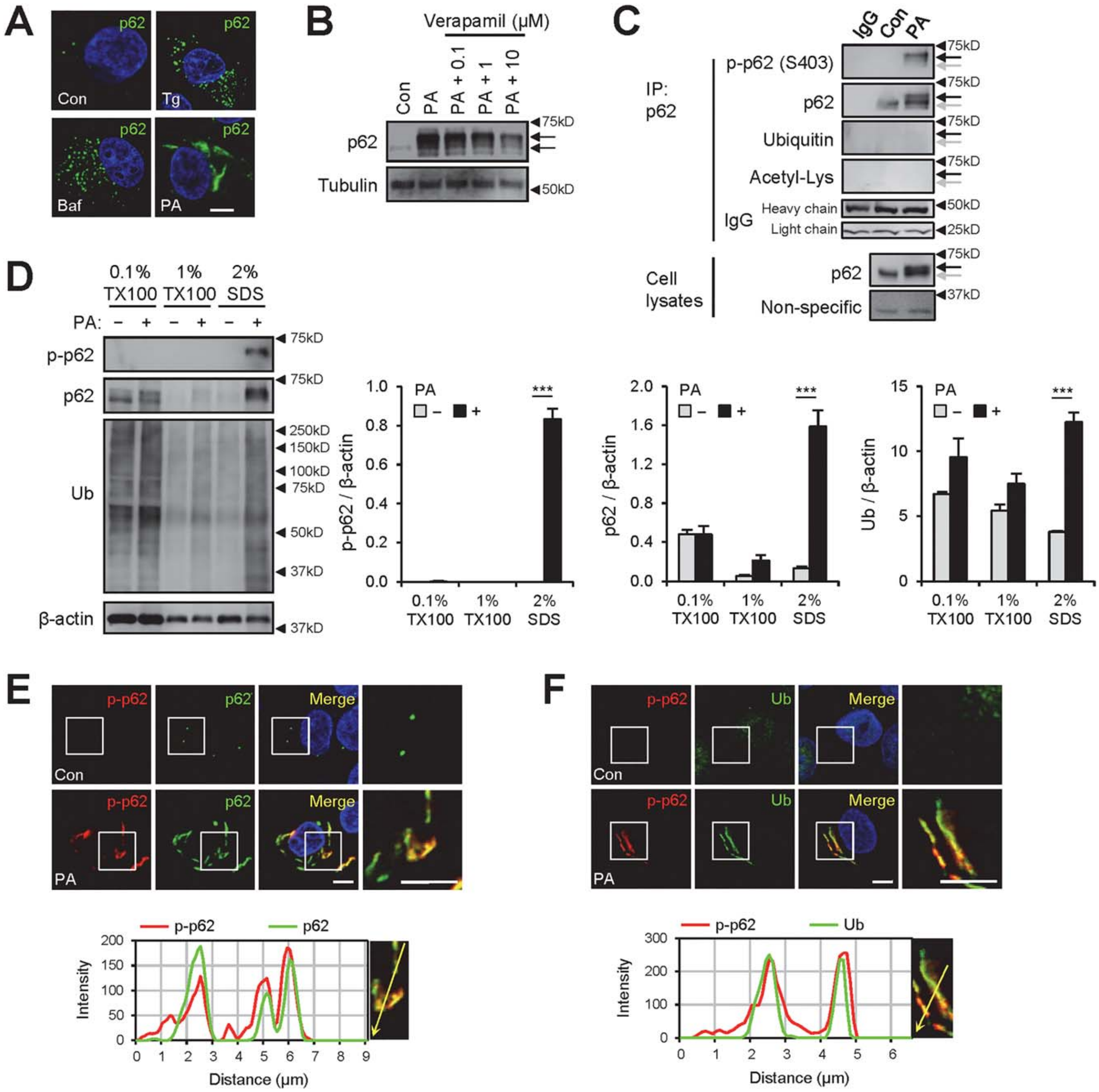

FIG. 1. SFA-induced lipotoxicity provokes p62/SQSTM1 phosphorylation in insoluble inclusion bodies. HepG2 cells were treated with BSA (Con), PA (500 μM), Tg (1 μM), Baf (100 nM), or PA + verapamil (0.1, 1, or 10 μM) for 9 hours and subjected to the following analyses. (A,B) Cells were subjected to immunostaining (A) and immunoblotting (B). Arrows indicate band shifts of p62. (C) PA-untreated (Con) and -treated cell lysates were subjected to immunoprecipitation (IP) using anti-p62 antibody or control immunoglobulin G (IgG). IP complex and whole-cell lysates were analyzed by immunoblotting. Background nonspecific and IgG chain bands were identified from p62 and ubiquitin blots, respectively, and used as loading controls. Arrows indicate positions of shifted (black) and unshifted (gray) p62 bands. (D) Cells were subjected to serial protein extraction (solubility fractionation) with indicated concentration of Triton X-100 (TX100) or SDS and analyzed by immunoblotting with indicated antibodies (left panel) and quantified (right panels). (E,F) Cells were subjected to immunostaining with indicated antibodies (upper panels) and analyzed by line-scan evaluation of each signal across protein inclusions (lower panels). DNA was stained with 4′,6-diamidino-2-phenylindole (blue). Boxed areas in fluorescence images are magnified in rightmost panels. Scale bars, 5 μm. Quantification data are shown as mean ± SEM. ***$P < 0.001$ (Student t test). Arrowheads indicate the exact or nearest position of the protein molecular-weight markers (kD).

signaling. To identify the nature of this modification, we immunoprecipitated p62 from SFA-treated cells and analyzed the protein with antibodies that detect various posttranslational modifications.

Ubiquitination and acetylation signals were not detected in the region corresponding to p62 bands (Fig. 1C), but we did find a strong phosphorylation signal on Ser403 of p62 after SFA treatment (Fig. 1C). This corresponded to the shifted p62 bands (Fig. 1C). The gel shift was reduced by treatment with both lambda protein phosphatase and calf intestinal phosphatase (Supporting Fig. S1B). Phosphorylated p62 was almost exclusively found in insoluble fractions (Fig. 1D) and colocalized with the protein inclusions consisting of p62 (Fig. 1E) and ubiquitinated proteins (Fig. 1F). SFA-induced p62 shift and phosphorylation was also prominently observed in freshly isolated primary mouse hepatocytes (Supporting Fig. S1C).

Autophagy inhibition and subsequent p62 accumulation can promote casein kinase 2 (CK2)-dependent p62 phosphorylation at Ser403.[21] Autophagy inhibitors Tg and Baf, however, produced very weak p62 Ser403 phosphorylation, in contrast to the strong p62 phosphorylation induced upon SFA treatment (Supporting Fig. S1D,E). Tetrabromobenzotriazole, a specific inhibitor of CK2,[21] did not inhibit SFA-induced p62 phosphorylation (Supporting Fig. S1F). These results indicate that neither autophagy inhibition nor CK2 is primarily responsible for SFA-induced p62 phosphorylation. Consistent with this, SFA-induced p62 phosphorylation occurred earlier than its total protein accumulation (Supporting Fig. S1G), suggesting that this phosphorylation is not simply attributed to increased protein accumulation and is likely an active process.

TBK1 IS ACTIVATED UPON SFA TREATMENT

We then tested whether TBK1, another p62 Ser403 kinase,[22] is responsible for SFA-induced p62 phosphorylation. SFA strongly activated TBK1 in HepG2 cells (Fig. 2A), as monitored by activation loop phosphorylation (Ser172) of TBK1. In contrast to SFA, Tg and Baf only induced moderate activation of TBK1 (Fig. 2A), consistent with the p62 phosphorylation results (Supporting Fig. S1D,E). Calcium-channel blockers verapamil and nicardipine did not inhibit SFA-induced TBK1 phosphorylation (Fig. 2B), although they strongly reduced p62 accumulation (Figs. 1B and 2B) by restoring autophagic flux.[15] Interestingly, UFAs, such as oleic acid (OA) and docosahexaenoic acid (DHA), almost completely inhibited the action of SFA in activating TBK1 (Fig. 2C) and inducing p62 phosphorylation and accumulation (Fig. 2D).

In cells, activated TBK1 (p-TBK1) colocalized with phosphorylated p62 (p-p62; Fig. 2E) and total p62 (Fig. 2F) inclusions, suggesting that TBK1 may be the kinase responsible for Ser403 phosphorylation of p62. However, unlike p-p62 that was predominantly found in the insoluble fraction (Fig. 1D), p-TBK1 was found in both soluble and insoluble fractions (Supporting Fig. S1H). One possibility is that TBK1 is present at the soluble side of the protein inclusion in order to efficiently phosphorylate p62 and assemble them into the insoluble inclusions. Consistent with this idea, PA-activated TBK1 phosphorylated p62 in an *in vitro* kinase assay (Supporting Fig. S1I) and can bind to endogenous p62 in reciprocal coimmunoprecipitation assays (Supporting Fig. S1J).

TBK1 IS REQUIRED FOR SFA-INDUCED p62 PHOSPHORYLATION AND ACCUMULATION

We were curious whether TBK1 actively promoted p62 phosphorylation and formation of ubiquitin-p62 aggregates in this lipotoxic context. Therefore, we used two recently discovered pharmacological inhibitors for TBK1: BX795[23] and amlexanox.[24] Both BX795 and amlexanox effectively suppressed SFA-induced p62 phosphorylation (Fig. 3A), supporting the hypothesis that TBK1 mediates the effect of SFA on p62 phosphorylation. Interestingly, SFA-induced accumulation of p62 and ubiquitinated proteins in insoluble fractions (Fig. 3A) and cytoplasmic inclusions (Fig. 3B) were also strongly inhibited, suggesting a relationship between p62 phosphorylation and protein inclusion formation.

Although BX795 and amlexanox are relatively specific inhibitors for TBK1, they may also inhibit other kinases such as phosphoinositide-dependent kinase 1 and inhibitory κB kinase ε.[23,24] To independently examine the role of TBK1, we used TBK1-specific short hairpin RNA (shRNA) constructs. shRNA-mediated silencing of TBK1 almost completely inhibited the SFA-stimulated phosphorylation of p62 (Fig. 3C), indicating that TBK1 is indeed the major kinase that phosphorylates p62 in response to SFA. TBK1 silencing also prevented accumulation of insoluble p62 and ubiquitinated proteins (Fig. 3C), suggesting that the TBK1 activation and subsequent phosphorylation of p62 is responsible for accumulation of insoluble protein aggregates in SFA-treated cells.

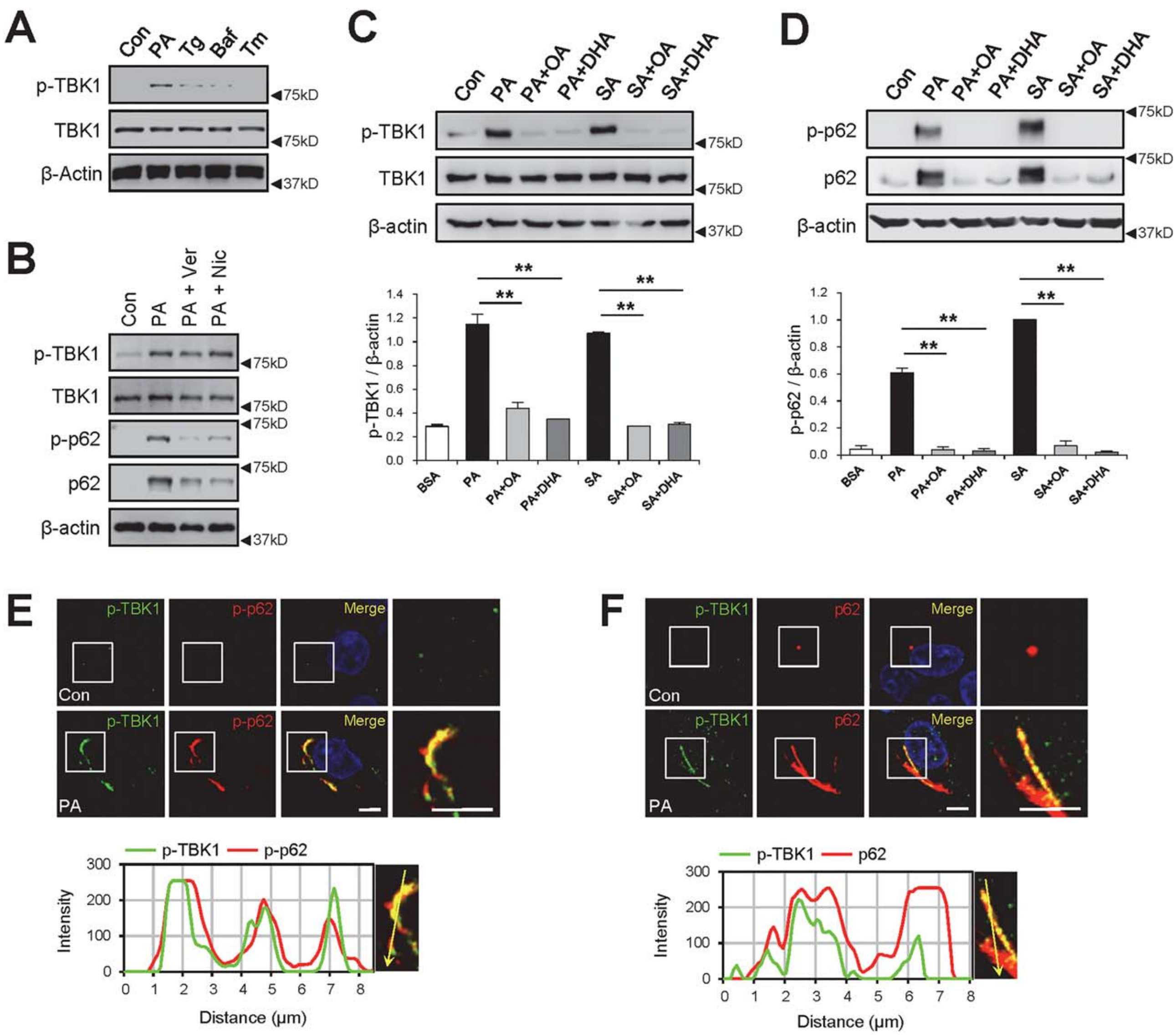

FIG. 2. SFA induces TBK1 activation and aggregation with phosphorylated p62. HepG2 cells were treated with BSA (Con), PA (500 μM), Tg (1 μM), Baf (100 nM), tunicamycin (Tm; 5 μg/mL), verapamil (Ver; 50 μM), nicardipine (Nic; 100 μM), SA (500 μM), OA (500 μM), and/or DHA (500 μM) for 9 hours, followed by immunoblotting (A-D), immunoblotting quantification (C,D; lower panels), and immunostaining (E,F). Immunostained images of PA-treated cells (upper panels) were analyzed by line-scan evaluation of each signal across protein inclusions (lower panels). Scale bars, 5 μm. Quantification data are shown as mean ± SEM. $^{**}P < 0.01$ (Student *t* test). Arrowheads indicate the exact or nearest position of the protein molecular-weight markers (kD).

THE CYCLIC GMP-AMP SYNTHASE/STIMULATOR OF INTERFERON GENES AXIS IS REQUIRED FOR SFA-INDUCED TBK1 ACTIVATION

Next, we explored the mechanism of how TBK1 is activated upon lipotoxic insult during obesity. We focused on stimulator of interferon genes (stimulator of interferon genes [STING]), a physiological activator of TBK1.[25] Unstimulated STING resides in the ER membrane, while upon stimulation with foreign DNA or cyclic dinucleotides, it translocates into an unknown cytoplasmic compartment where it interacts with TBK1 and induces TBK1 activation.[25] Notably, lipid composition of the ER membrane is dramatically

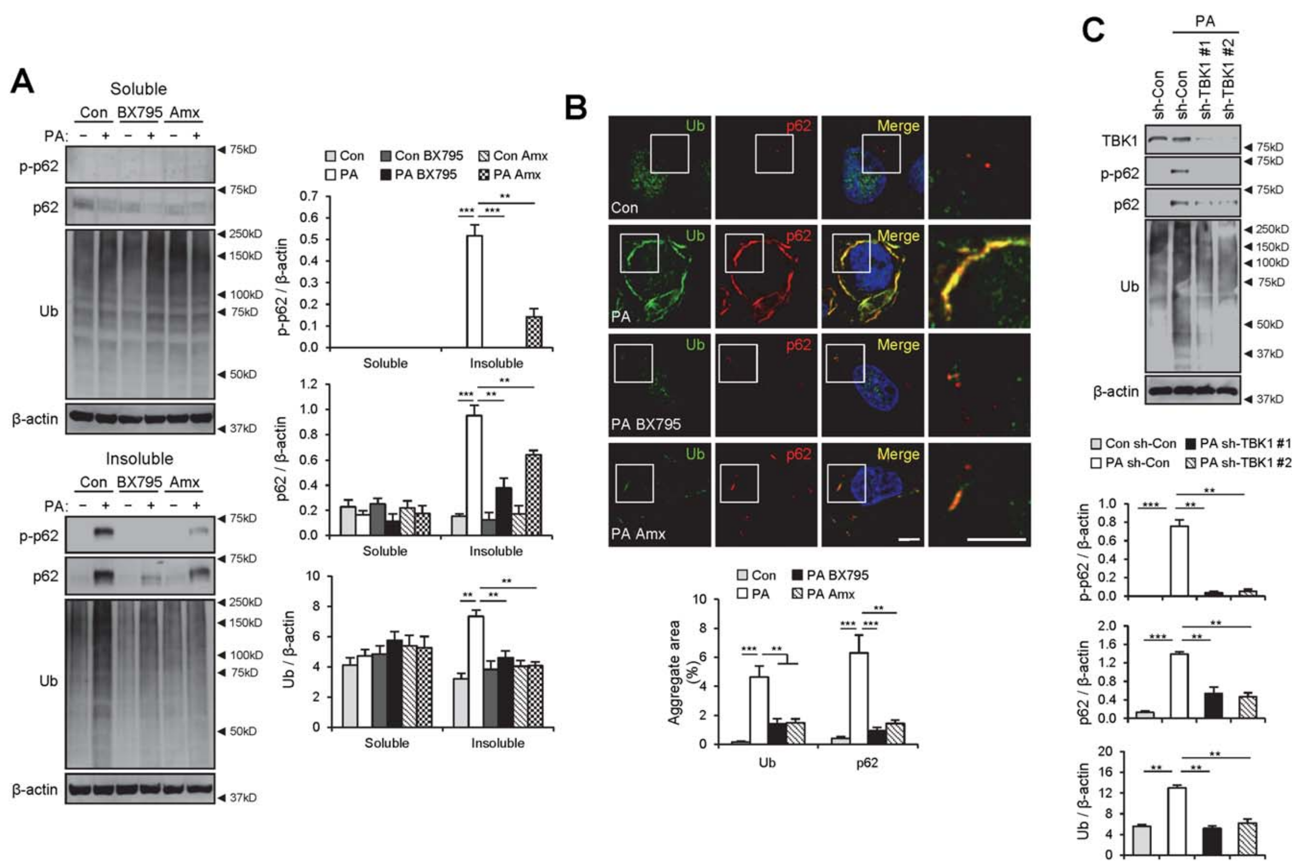

FIG. 3. TBK1 mediates SFA-induced p62 phosphorylation and aggregation into ubiquitinated protein inclusions. (A,B) HepG2 cells were treated with BSA (Con), PA (500 μM), BSA + BX795 (20 μM), PA + BX795, BSA + Amlexanox (Amx; 100 μM), or PA + Amx for 9 hours. (A) Cells were lysed, fractionated into 1% Triton X-100-soluble and -insoluble fractions, and then subjected to immunoblotting (left panels) and immunoblotting quantification (right panels). (B) Cells with indicated treatments were subjected to immunostaining (upper panel). Boxed areas in fluorescence images are magnified in rightmost panels. Amount of aggregated proteins was quantified (lower panel). Scale bars, 5 μm. (C) HepG2 cells were transduced with shRNA lentiviruses targeting luciferase (sh-Con) or TBK1 (sh-TBK1 #1 and #2) and incubated for 48 hours. Then, cells were treated with BSA or PA (500 μM) for 9 hours, followed by subcellular fractionation, immunoblotting (upper panel), and immunoblotting quantification (lower panels). TBK1 was analyzed from soluble fractions while p62, ubiquitin, and β-actin were analyzed from insoluble fractions. All data are shown as mean ± SEM. **$P < 0.01$; ***$P < 0.001$ (Student t test). Arrowheads indicate the exact or nearest position of the protein molecular-weight markers (kD).

altered during SFA-induced lipotoxicity,[26] and lipid modification (palmitoylation) of STING is required for its activation.[27] Under SFA-induced lipotoxicity, STING was found to colocalize with p-TBK1 (Fig. 4A), and shRNA-mediated silencing of STING substantially decreased SFA-induced TBK1 activation (Fig. 4A,B and Supporting Fig. S2A,B). STING silencing was also sufficient to prevent SFA-induced p62 phosphorylation and ubiquitin-p62 inclusions (Fig. 4B and Supporting Fig. S2A-D), supporting the idea that the STING-TBK1 axis mediates SFA-induced p62 phosphorylation and aggregation in hepatocytes.

Cyclic GMP-AMP (cGAMP), an upstream regulator of STING, can be synthesized in animal cells by the action of cGAMP synthase (cGAS). cGAS is activated by the presence of cytoplasmic DNA, which could result from viral infection[28] or mitochondrial collapse.[29,30] Importantly, lipotoxic damage and NASH are associated with mitochondrial dysfunction and cytoplasmic leakage of mitochondrial DNA,[31,32] which can activate cGAS and subsequently the STING-TBK1 axis. Indeed, shRNA-mediated silencing of cGAS decreased SFA-induced TBK1 activation (Fig. 4C,D). cGAS silencing also inhibited p62 phosphorylation (Fig. 4D and Supporting Fig. S3A,B), STING translocation to the p-

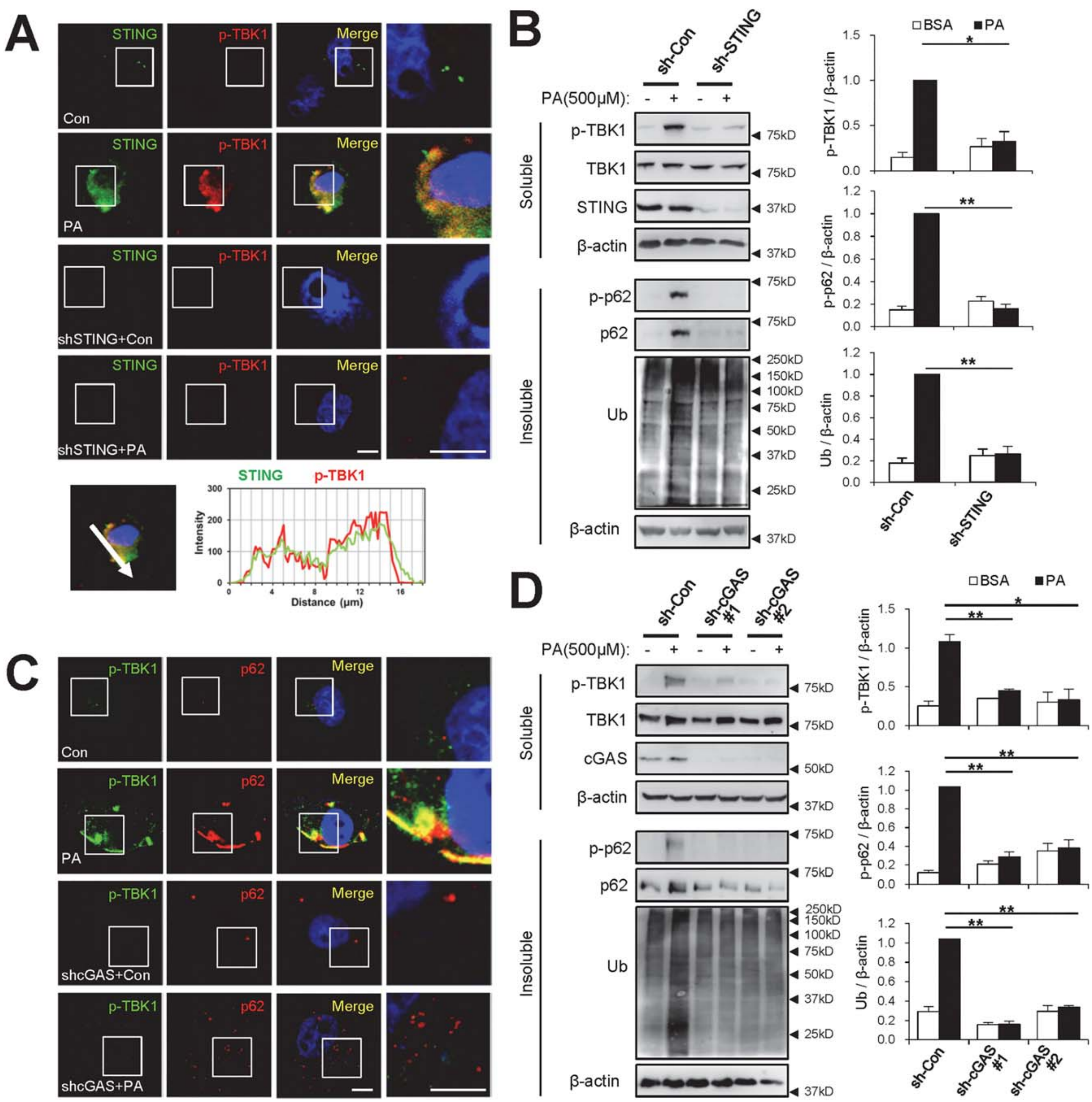

FIG. 4. The cGAS-STING axis mediates SFA-induced activation of TBK1. At 48 hours after infection with shRNA lentiviruses for luciferase (sh-Con), STING (sh-STING), or cGAS (sh-cGAS#1 and #2), HepG2 cells were treated with BSA (Con) or PA (500 μM) for 9 hours. Then, cells were subjected to immunostaining (A,C), subcellular fractionation and immunoblotting (B,D; left panels), and immunoblotting quantification (B,D; right panels). Boxed areas in fluorescence images are magnified in rightmost panels. Immunostained images of PA-treated control cells (A, upper panel) were analyzed by line-scan evaluation of each signal across protein inclusions (A, lower panel). Scale bars, 5 μm. Quantification data are shown as mean ± SEM. *$P < 0.05$; **$P < 0.01$ (Student t test). Arrowheads indicate the exact or nearest position of the protein molecular-weight markers (kD).

TBK1-positive compartment (Supporting Fig. S3C,D), and accumulation of ubiquitin-p62 inclusions (Fig. 4C,D and Supporting Fig. S3A-D). These results indicate that cGAS is necessary for SFA-induced activation of the STING-TBK1 axis and subsequent p62 phosphorylation and aggregation.

Although cGAS activation is necessary for activating the TBK1 axis during SFA-induced lipotoxicity, it was not sufficient for inducing p62 inclusion. For instance, TBK1 activation by extracellular cGAMP[28] (Supporting Fig. S4A) did not provoke p62 phosphorylation and accumulation in cells (Supporting Fig. S4B). Therefore, activation of additional SFA-induced signaling pathways seems to be necessary for TBK1 to properly induce p62 phosphorylation and aggregation.

We tested whether the requirement of STING and cGAS for activating the TBK1-p62 axis could be replicated in primary mouse hepatocytes, using *Sting*- and *cGas*-knockout mice.[28] As observed in HepG2 cells, PA-induced lipotoxicity in wild-type (WT) mouse hepatocytes triggered strong phosphorylation of TBK1 (Supporting Fig. S5A) and p62 (Supporting Fig. S5B) in protein inclusions. However, primary hepatocytes isolated from *Sting*- and *cGas*-knockout mice exhibited dramatic attenuation of these processes in both immunostaining (Supporting Fig. S5A,B) and immunoblotting (Supporting Fig. S5C-F) experiments. These results support the requirement of the cGAS-STING axis in lipotoxicity-induced TBK1 activation and subsequent induction of p62-ubiquitinated protein inclusions.

TBK1 CONTROLS NUCLEAR FACTOR ERYTHROID 2-RELATED FACTOR 2 TARGETS AND AUTOPHAGIC FLUX

Excessive accumulation of p62 can up-regulate the nuclear factor erythroid 2-related factor 2 (Nrf2) transcription factor because p62 inhibits Kelch-like ECH-associated protein 1, an Nrf2 suppressor.[33] *SQSTM1*, the gene encoding p62, is also a transcriptional target of Nrf2; therefore, p62 accumulation leads to further up-regulation of p62 expression, forming a positive feedback loop.[33] Consistent with this pathway, SFA induced strong expression of Nrf2 target genes, including *SRX*, *NQO1*, *GSTA1*, and *SQSTM1* (Supporting Fig. S6A-D). Silencing of *cGAS*, *STING*, or *TBK1* abolished the lipotoxicity-induced Nrf2 target gene expression (Supporting Fig. S6A-D), whereas silencing of p62/SQSTM1 did not inhibit lipotoxicity-induced TBK1 activation (Supporting Fig. S6E). These results indicate that, in the context of lipotoxicity, TBK1 acts as an upstream regulator of p62 and other Nrf2 target genes.

As we formerly reported,[15] PA-induced lipotoxicity provoked an almost complete segregation between an autophagosome marker, microtubule-associated protein light chain 3 (LC3), and a lysosomal marker, lysosome-associated membrane protein 1 (LAMP1; Supporting Fig. S7A,B), indicating a strong autophagy arrest at the autophagosomal-lysosomal fusion step. TBK1 inhibitors, BX795 and amlexanox, were able to substantially restore the colocalization between LC3 and LAMP1 (Supporting Fig. S7A,B), indicating that they can, at least partially, resume autophagic flux during lipotoxicity. As a result of efficient lysosomal fusion and subsequent degradation, the level of LC3-positive autophagosomes was reduced by the TBK1 inhibitors (Supporting Fig. S7C). It is possible that reduced p62 expression and aggregation during TBK1 inhibition may have lessened the autophagy overload and thereby alleviated the autophagic defects. Restoration of autophagic flux may have further contributed to efficient elimination of p62 and ubiquitinated protein inclusions (Fig. 3) as a positive feedback.

TBK1 INHIBITION SUPPRESSES PROTEIN INCLUSIONS IN LIVERS OF OBESE MICE

Next, we examined whether TBK1 is important for p62 control *in vivo* during HFD-induced fatty liver.[13-15] As observed in SFA-treated HepG2 cells, insoluble p62 induced by HFD was phosphorylated at Ser403 (Fig. 5A). Ten days of TBK1 inhibition by BX795 administration was sufficient to reduce this phosphorylation, suggesting a mechanistic role of TBK1 in HFD-induced p62 phosphorylation (Fig. 5A). The level of p62 and ubiquitinated proteins in hepatic inclusion bodies was also dramatically reduced to the level of preobese conditions (Fig. 5A,B), indicating that TBK1 is indeed important for p62 regulation during obesity. However, BX795 was also found to substantially reduce body weight without altering food intake (Supporting Fig. S8A,B). Because systemic TBK1 inhibition is known to control energy metabolism and inflammation through adipose tissues,[24,34] it is possible that these inhibitors corrected the HFD-induced protein inclusion pathologies indirectly through suppression of obesity and normalization of metabolism.

To address this issue, we generated liver-specific TBK1-knockout (L-*Tbk1*-KO) mice by crossing *Tbk1*$^{F/F}$ mice with the *Albumin-Cre* strain. As expected, L-*Tbk1*-KO mice exhibited dramatically reduced expression of both p-TBK1 and TBK1 in liver tissue (Fig. 5C). However, HFD-induced body weight gain was almost the same between L-*Tbk1*-KO mice and L-*Tbk1*-WT (*Tbk1*$^{F/F}$; littermate control) mice (Supporting Fig. S8C,D), suggesting that the effect of liver-

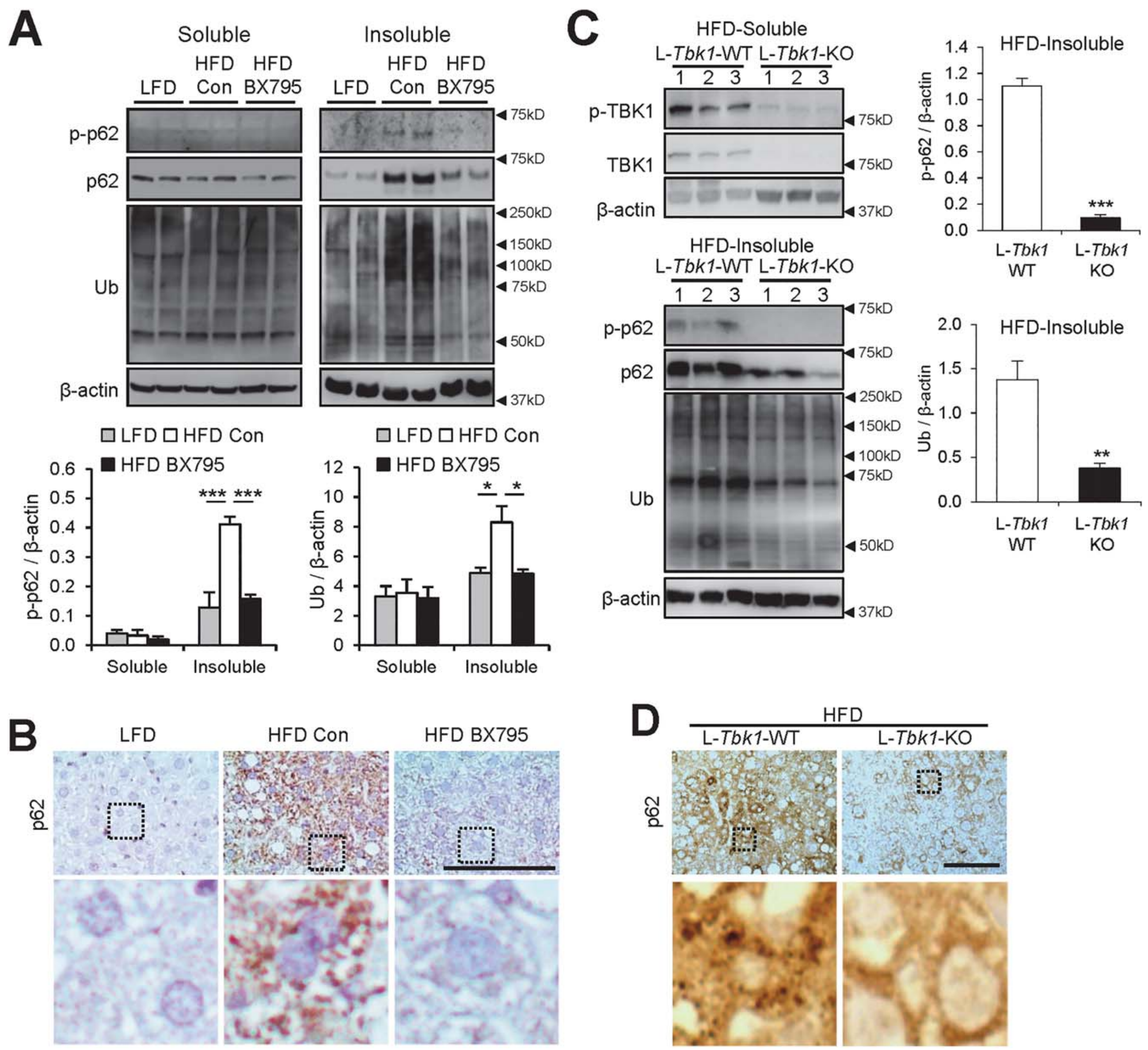

FIG. 5. Inhibition of TBK1 suppresses p62 phosphorylation and accumulation in livers of obese mice. (A,B) Four-month-old C57BL/6 male mice kept on HFD for 2 months were subjected to daily administration of phosphate-buffered saline (Con; n = 7) or BX795 (25 mg/kg body weight, intraperitoneal; n = 6) for 10 days. LFD-kept mice (n = 5) of the same age were used as a negative control. (C,D) Five-month-old littermate-controlled $Tbk1^{F/F}$ (n=16) and $Albumin\text{-}Cre/Tbk1^{F/F}$ (n=16) male mice of C57BL/6 background, kept on HFD for 3 months, were analyzed. (A,C) Livers were subjected to solubility fractionation. One percent Triton X-100-soluble and -insoluble fractions were analyzed by immunoblotting and immunoblotting quantification. (B,D) Liver sections were subjected to p62 immunostaining. Hematoxylin counterstaining was used to visualize nuclei. Boxed areas in top panels are magnified in bottom panels. Scale bars, 200 μm. All data are shown as mean ± SEM. *$P < 0.05$; **$P < 0.01$; ***$P < 0.001$ (Student t test). Arrowheads indicate the exact or nearest position of the protein molecular-weight markers (kD).

specific TBK1 loss on general metabolism is minimal. Then, we analyzed the effect of L-*Tbk1*-KO on hepatic protein inclusions. Despite the minimal effects on obesity development (Supporting Fig. S8C,D), liver-specific TBK1 deletion dramatically reduced p62 phosphorylation (Fig. 5C), as well as accumulation of p62 and ubiquitinated proteins in insoluble inclusion bodies (Fig. 5C,D). These results demonstrate that TBK1 is indeed critical for obesity-induced p62 phosphorylation and subsequent formation of ubiquitin-p62 inclusions.

TBK1 INHIBITION REDUCES p62 INCLUSIONS AND LIVER FIBROSIS DURING NASH

Although HFD induces modest p62 inclusion formation (Fig. 5A,B),[13-15] HFD feeding in WT mice did not produce typical NASH pathologies such as active steatohepatitis or fibrotic lesions.[17] Therefore, HFD is combined with additional insults, such as nutritional deficiency[10,11] or expression of foreign proteins,[5,12] to induce a stronger NASH phenotype. These NASH models often produce much stronger accumulation of p62 and ubiquitinated proteins when compared to the simple HFD model.[5] Therefore, we tested the role of TBK1 in a more severe NASH model, induced by a methionine-restricted choline-deficient (CD)-HFD,[11] which recapitulates many of the human NASH pathologies.[11] These include severe hepatosteatosis and liver fibrosis (Supporting Fig. S9A), attenuated weight gain (Supporting Fig. S9B), and extensive liver damage (Supporting Fig. S9C). These pathologies were strongly suppressed by dietary supplementation of choline and methionine (CS-HFD; Supporting Fig. S9A-C).

We found that this CD-HFD model produced much stronger accumulation of phosphorylated p62 proteins (Fig. 6A), compared to the low-fat diet (LFD) or CS-HFD control animals (Supporting Fig. S9D). Correspondingly, accumulation of p62 and ubiquitinated proteins was also very pronounced in the CD-HFD model (Fig. 6A and Supporting Fig. S9D).

As observed in the simple HFD model (Fig. 5A), a 10-day treatment of the TBK1 inhibitor, BX795, was sufficient to suppress p62 phosphorylation and accumulation, as well as ubiquitinated protein inclusions (Fig. 6A) in the CD-HFD model. In this case, reduction in p62 inclusions was not associated with any significant changes in body weight (Supporting Fig. S9E) or level of hepatic fat accumulation (Fig. 6B and Supporting Fig. S9F). Levels of liver damage (Fig. 6C), hepatocyte cell death (Fig. 6D and Supporting Fig. S9F), and hepatic macrophage infiltration (Fig. 6D,E) were also comparable between BX795-untreated and -treated groups.

However, interestingly, we found that CD-HFD-induced expression of inflammatory cytokines, such as TNF1, interleukin (IL) 6 and IL10, was substantially suppressed by BX795 treatment (Supporting Fig. S9G). Furthermore, level of liver fibrosis, monitored through Sirius Red staining (Fig. 7A,B) and α-smooth muscle actin (α-SMA) expression (Fig. 7A-E), was substantially reduced by the BX795 treatment. Other markers of liver fibrosis, such as collagen (COL) levels (COL1A1 and COL3A1) and profibrogenic markers of hepatic stellate cells (e.g., matrix metalloproteinases [MMPs], tissue inhibitors of metalloproteinase [TIMPs], lysyl oxidase [LOX], connective tissue growth factor [CTGF], and platelet endothelial cell adhesion molecule 1 [PECAM-1]), were also induced by CD-HFD and suppressed by BX795 treatment (Fig. 7C-E).

TBK1 INHIBITION REDUCES NASH-ASSOCIATED REACTIVE OXYGEN SPECIES ACCUMULATION

Suppression of TBK1 and subsequent inhibition of p62 protein inclusions (Fig. 6A,B) did not alleviate liver damage and hepatocyte death (Fig. 6C,D). However, given that TBK1 inhibition strongly reduced fibrotic pathologies (Fig. 7A-E), it is still possible that hepatic p62 protein inclusions somehow contribute to fibrotic pathologies by inducing sublethal damages in hepatocytes. One such hepatocyte-originated signal is reactive oxygen species (ROS) that provoke hepatic stellate cell activation.[35,36] Indeed, in a recent report, hepatocyte-specific knockout of p62, which inhibits protein inclusion formation, strongly suppressed ROS accumulation and fibrosis during NASH.[12] We tested whether TBK1 inhibition, which suppresses p62 inclusion (Fig. 6A,B), can also reduce ROS accumulation during CD-HFD-induced NASH. ROS visualization using dihydroethidium (DHE) revealed that, as expected, CD-HFD prominently up-regulated liver ROS level, whereas BX795 treatment strongly antagonized the effect of CD-HFD (Fig. 8A,B). Therefore, TBK1 inhibition effectively suppressed hepatic oxidative stress and fibrosis during NASH.

STING IS INVOLVED IN HFD-INDUCED p62 PHOSPHORYLATION

We then tested the genetic involvement of the cGAS-STING pathway in the mouse NASH models. Upon the simple HFD treatment, *Sting*-KO mice produced less p62 phosphorylation and accumulation

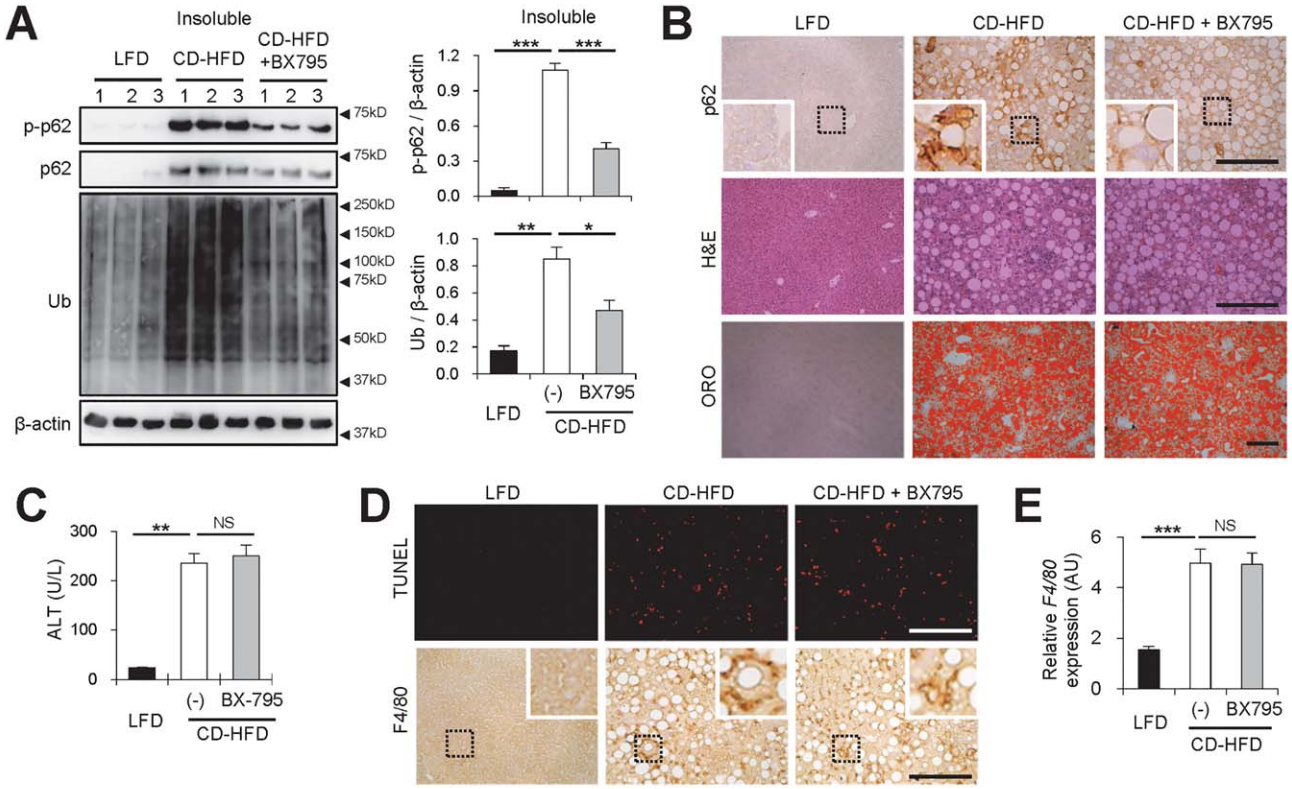

FIG. 6. Inhibition of TBK1 suppresses NASH-associated p62 phosphorylation and protein inclusion without alleviating hepatosteatosis and liver damage. (A-E) Four-month-old C57BL/6 male mice kept on CD-HFD for 2 months were subjected to daily administration of vehicle (Con; 5% Tween-80 and 5% PEG-400; n = 10) or BX795 (25 mg/kg body weight, intraperitoneal; n = 5) for 10 days. LFD-kept mice (n = 5) of the same age were used as a negative control. (A) Livers were subjected to solubility fractionation. One percent Triton X-100-insoluble fractions were analyzed by immunoblotting (left panel) and immunoblotting quantification (right panels). (B,D) Liver sections were subjected to p62 and F4/80 immunostaining, hematoxylin and eosin (H&E) staining, Oil Red O (ORO) staining, and terminal deoxynucleotidyl transferase dUTP Nick-End Labeling (TUNEL) staining. Hematoxylin counterstaining was used to visualize nuclei. Scale bars, 200 μm. Boxed areas are magnified in the insets. (C) Serum ALT levels were quantified. (E) Relative F4/80 expression was quantified through RT-PCR. All data are shown as mean ± SEM. NS, not statistically significant; $^{*}P < 0.05$; $^{**}P < 0.01$; $^{***}P < 0.001$; Student *t* test). Arrowheads indicate the exact or nearest position of the protein molecular-weight markers (kD).

when compared to WT mice (Supporting Fig. S10A, B) without significant effects on obesity development (Supporting Fig. S10D,E). Accumulation of ubiquitinated proteins was also much less pronounced in *Sting*-KO mice (Supporting Fig. S10A,C), suggesting a role for STING in the p62 phosphorylation and protein inclusion processes. However, under the CD-HFD treatment, the effect of STING loss was not detectable (Supporting Fig. S10F-H). Therefore, even though the cGAS-STING pathway plays important roles in activating TBK1 upon lipotoxic stimuli, other types of metabolic insults such as choline deficiency and liver damage can activate additional independent signaling pathway(s) that can provoke activation of the TBK1-p62 signaling.

Discussion

The hepatocyte protein inclusion is one of the most prominent histopathological features of diseased hepatocytes in fatty liver,[3-5,7-9] in addition to steatosis and cell death. The association between fatty liver pathologies and inclusion bodies has been known for around 100 years, and ubiquitinated proteins and p62/SQSTM1 were more recently shown to be the major

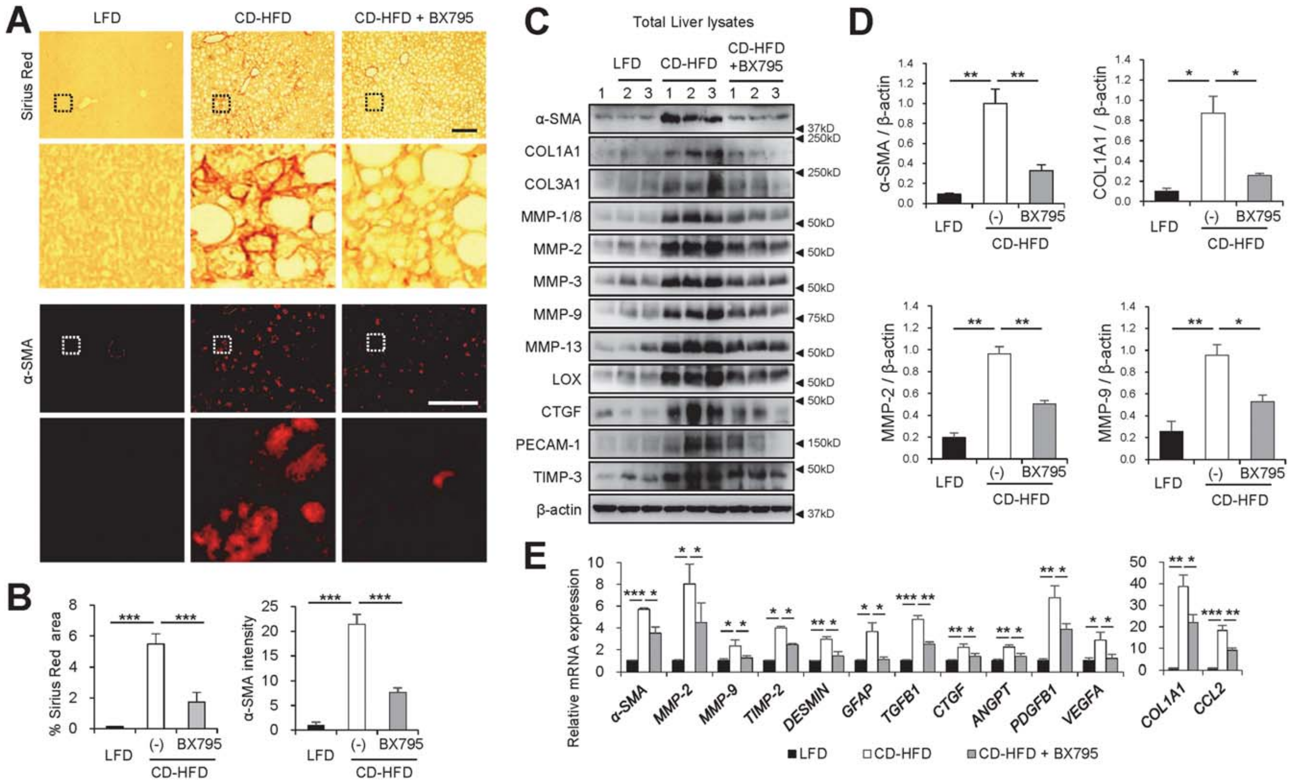

FIG. 7. Inhibition of TBK1 suppresses liver fibrosis induced by NASH. (A-E) Mice described in Fig. 6 were also analyzed by the following experiments. (A) Liver sections were subjected to Sirius Red staining and α-SMA immunostaining. Scale bars, 200 μm. Boxed areas are magnified in the bottom panel. (B) Areas positive for Sirius Red (left panel) or α-SMA fluorescence intensity (right panel) were quantified. (C,D) Total liver lysates were analyzed by immunoblotting (C) and immunoblotting quantification (D). (E) Relative mRNA expression was quantified through RT-PCR. All data are shown as mean ± SEM. *$P < 0.05$; **$P < 0.01$; ***$P < 0.001$ (Student t test). Arrowheads indicate the exact or nearest position of the protein molecular-weight markers (kD).

components.[3,8] Still, whether these p62 inclusions indeed play a pathogenetic role, and the mechanisms of how these inclusion bodies form during lipotoxic injuries, largely remained elusive until very recently. In addition to recent studies that showed the pathogenetic role for p62 inclusions during autophagy inhibition, NASH, and HCC,[12,37] our current study provides a mechanism for how p62 protein inclusions can form inside lipid-laden hepatocytes during fatty liver and NASH.

We demonstrate here that SFA- or obesity-induced lipotoxicity promotes protein inclusion formation through activation of the TBK1 signaling pathway. Also referred to as the xenophagy pathway, the TBK1 axis has been known to facilitate autophagic elimination of invading microorganisms in macrophages (Fig. 8C).[22] In this process, TBK1, activated by bacterially derived lipopolysaccharide, cyclic dinucleotides, or DNA, phosphorylates p62 at Ser403 and subsequently promotes its association with ubiquitinated bacterial proteins, forming bacteria-p62 aggregates that are destined for autophagic degradation. Here, we showed that the same pathway plays a distinct pathogenetic role in hepatocytes during obesity-associated NASH. Upon lipotoxic insults, TBK1 is activated by the cGAS-STING pathway, as well as by unknown signaling mediators (Fig. 8D). Activated TBK1 phosphorylates p62 at Ser403, promoting the formation of ubiquitinated protein inclusions. Although this process normally functions to prepare ubiquitinated proteins for autophagic degradation, obesity and lipotoxic injuries interfere with autophagic flux through an independent mechanism.[13,15] Therefore, protein inclusions that cannot be degraded by either autophagy or proteasomal pathways accumulate and grow larger in size. p62 phosphorylation and accumulation further up-

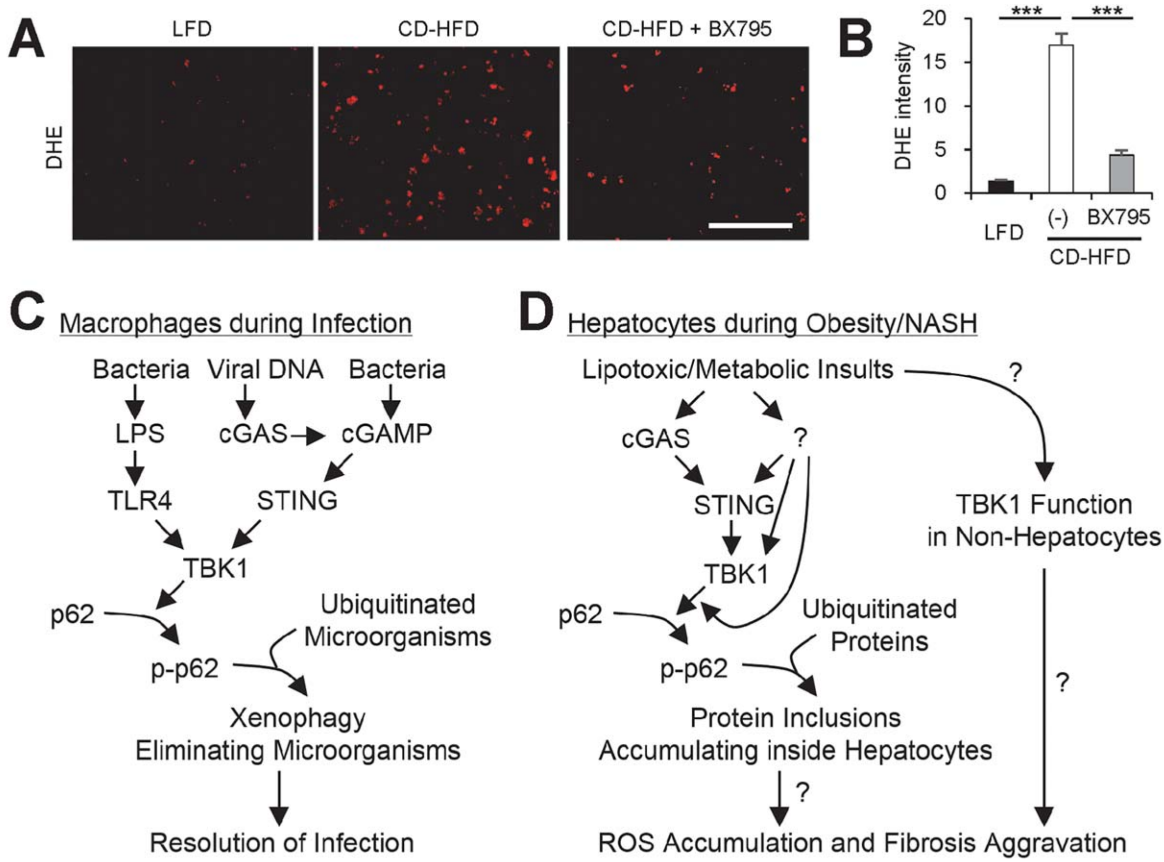

FIG. 8. Inhibition of TBK1 suppresses hepatic oxidative stress during NASH. (A) Fresh frozen liver sections from mice described in Fig. 6 were analyzed by DHE staining, which visualizes ROS. Scale bars, 200 μm. (B) DHE fluorescence intensity was quantified. Data are shown as mean ± SEM. $^{***}P < 0.001$ (Student *t* test). (C) During infection, TBK1-dependent p62 phosphorylation induces aggregation of ubiquitinated microorganisms, making them better substrates for autophagy, which leads to quicker microorganism elimination. (D) During obesity and NAFLD, lipotoxic activation of TBK1 signaling provokes the formation of p62-ubiquitin aggregates. Because of autophagy defects, hepatocytes cannot efficiently eliminate these aggregates, leading to the formation of large protein inclusions during NASH. These protein inclusions can provoke sublethal ROS accumulation, which can culminate in the development of fibrosis during NASH. In addition, lipotoxicity may also increase TBK1 signaling in nonhepatocytes, such as hepatic stellate cells and immune cells, which may contribute to the fibrotic pathologies. Question marks denote the mechanistic connections that still need to be established by future investigations.

regulates p62 expression through Nrf2-mediated positive feedback,[33] which aggravates autophagy overload and malfunctioning. These results provide a mechanistic explanation of how p62 inclusions form during lipotoxic injuries and fatty liver. Even though more studies need to be done on how these inclusions are mechanistically associated with other pathological features of NASH, we believe that this study, delineating the mechanisms of how lipotoxic injuries provoke p62 protein inclusions, is an important advance in the field of NASH and fatty liver diseases.

Because p62 is known to regulate redox homeostasis, nutrient signaling, and carcinogenic processes,[16] lipotoxic p62 phosphorylation and accumulation may play additional pathogenetic roles in fatty liver disease. Indeed, our results indicate that TBK1 inhibition, which suppresses p62 phosphorylation and accumulation, can specifically restore liver ROS accumulation and subsequent fibrotic pathologies in a NASH model induced by CD-HFD. However, other NASH-associated pathologies, such as hepatosteatosis, hepatocyte damage, and macrophage infiltration, were not altered by TBK1 inhibition in this model. Interestingly, recent studies of hepatocellular p62 indicated that hepatocyte-specific p62 knockout mice, which do not form hepatic protein inclusions, showed the exact same phenotype; p62 ablation suppressed liver ROS and fibrosis without alleviating hepatosteatosis during NASH.[12] Because both TBK1 inhibition and p62 ablation suppresses protein inclusion formation, oxidative stress, and fibrosis, it is plausible that the protein inclusions play a pathogenetic role in redox imbalance and subsequent fibrotic progression. For instance, aberrant accumulation of protein inclusions and subsequent block of autophagy can impair the clearance of dysfunctional mitochondria that produce pathogenic levels of ROS. However, the exact mechanism for how p62 inclusions provoke a redox imbalance in the liver during NASH was not provided by either the former studies or the current study. Therefore, future investigation should work toward extensively understanding this potential mechanism. In addition, considering that TBK1 has a well-established role in regulating inflammatory signaling,[38] it is possible that the observed effects on liver fibrosis were mediated through p62-independent mechanisms in nonhepatocytes such as macrophages or hepatic stellate cells. Although damaged hepatocytes are among the major sources of ROS during NASH, other cell types, such as immune cells, could also contribute to the ROS production.[36] Therefore, even though it is likely that hepatic protein inclusions are specific promoters of liver fibrosis and that TBK1 is a central signaling component for this NASH-promoting process, alternative explanations are possible through the role of TBK1-expressing nonhepatocytes (Fig. 8D).

Excessive p62 protein inclusions in NASH predispose a patient to HCC progression, and HCC with prominent p62 inclusions predicts a poor prognostic outcome.[12,39,40] Therefore, the p62 protein inclusions may also have a role in promoting liver cancer. Indeed, recent animal studies established that the homeostatic maintenance of p62 levels in liver tumors and tumor microenvironments is important for suppressing hepatocarcinogenesis.[12,16,33,41] Specifically, p62 accumulation in hepatocytes promotes HCC development during NASH,[12] whereas endogenous p62 in hepatic stellate cells suppresses HCC by modulating the tumor microenvironment.[41] Given that our results show that obesity-activated TBK1 signaling plays a critical role in producing p62 inclusion accumulation in hepatocytes during lipotoxicity, it may provide the molecular conduit of how hypernutrition and obesity can promote NASH-associated development of HCC.[6]

It should be noted that pharmacological TBK1 inhibition was recently shown to alleviate NAFLD and insulin resistance in both humans and mice,[24,42] which is likely to be mediated by the inflammation-regulating role of TBK1 in adipose tissues and macrophages.[24,34,38] In addition to these well-established roles in inflammation, our current study shows that TBK1 also plays an important role for protein homeostasis in hepatocytes through regulating p62 phosphorylation. TBK1 inhibition and subsequent suppression of hepatic protein inclusions might also contribute to restoring liver redox homeostasis and attenuating fibrotic disease progression. Therefore, further investigation about how the TBK1 pathway is regulated by lipotoxic insults and how TBK1 regulation in different tissues affects various pathologies in NASH may bring about a new paradigm for understanding NAFLD, as well as other similar types of liver diseases that present with the disruption of protein homeostasis.

Acknowledgments: We thank Drs. L. Yin and D. Zhang for primary hepatocyte isolation. We thank Drs. M.B. Omary and S. Hwang (University of Chicago) and Lee lab members for their insightful comments. We also thank Drs. R.A. Miller and S. Pletcher for access to lab equipment and Santa Cruz Biotech Inc. for sharing reagents.

REFERENCES

1) Scherer PE, Hill JA. Obesity, diabetes, and cardiovascular diseases: a compendium. Circ Res 2016;118:1703-1705.
2) Cusi K. Role of obesity and lipotoxicity in the development of nonalcoholic steatohepatitis: pathophysiology and clinical implications. Gastroenterology 2012;142:711-725.e6.
3) Zatloukal K, Stumptner C, Fuchsbichler A, Heid H, Schnoelzer M, Kenner L, et al. p62 Is a common component of cytoplasmic inclusions in protein aggregation diseases. Am J Pathol 2002; 160:255-263.
4) Strnad P, Nuraldeen R, Guldiken N, Hartmann D, Mahajan V, Denk H, Haybaeck J. Broad spectrum of hepatocyte inclusions in humans, animals, and experimental models. Compr Physiol 2013;3:1393-1436.
5) Kucukoglu O, Guldiken N, Chen Y, Usachov V, El-Heliebi A, Haybaeck J, et al. High-fat diet triggers Mallory-Denk body formation through misfolding and crosslinking of excess keratin 8. HEPATOLOGY 2014;60:169-178.
6) **Marengo A**, **Rosso C**, Bugianesi E. Liver cancer: connections with obesity, fatty liver, and cirrhosis. Annu Rev Med 2016;67: 103-117.
7) Caldwell S, Ikura Y, Dias D, Isomoto K, Yabu A, Moskaluk C, et al. Hepatocellular ballooning in NASH. J Hepatol 2010;53: 719-723.
8) Stumptner C, Fuchsbichler A, Heid H, Zatloukal K, Denk H. Mallory body–a disease-associated type of sequestosome. HEPATOLOGY 2002;35:1053-1062.

9) **Brunt EM**, **Tiniakos DG**. Histopathology of nonalcoholic fatty liver disease. World J Gastroenterol 2010;16:5286-5296.
10) Rinella ME, Elias MS, Smolak RR, Fu T, Borensztajn J, Green RM. Mechanisms of hepatic steatosis in mice fed a lipogenic methionine choline-deficient diet. J Lipid Res 2008;49:1068-1076.
11) Matsumoto M, Hada N, Sakamaki Y, Uno A, Shiga T, Tanaka C, et al. An improved mouse model that rapidly develops fibrosis in non-alcoholic steatohepatitis. Int J Exp Pathol 2013;94:93-103.
12) Umemura A, He F, Taniguchi K, Nakagawa H, Yamachika S, Font-Burgada J, et al. p62, Upregulated during preneoplasia, induces hepatocellular carcinogenesis by maintaining survival of stressed HCC-initiating cells. Cancer Cell 2016;29:935-948.
13) Gonzalez-Rodriguez A, Mayoral R, Agra N, Valdecantos MP, Pardo V, Miquilena-Colina ME, et al. Impaired autophagic flux is associated with increased endoplasmic reticulum stress during the development of NAFLD. Cell Death Dis 2014;5:e1179.
14) **Yang L**, **Li P**, Fu S, Calay ES, Hotamisligil GS. Defective hepatic autophagy in obesity promotes ER stress and causes insulin resistance. Cell Metab 2010;11:467-478.
15) Park HW, Park H, Semple IA, Jang I, Ro SH, Kim M, et al. Pharmacological correction of obesity-induced autophagy arrest using calcium channel blockers. Nat Commun 2014;5:4834.
16) Moscat J, Karin M, Diaz-Meco MT. p62 in cancer: signaling adaptor beyond autophagy. Cell 2016;167:606-609.
17) Park HW, Park H, Ro SH, Jang I, Semple IA, Kim DN, et al. Hepatoprotective role of Sestrin2 against chronic ER stress. Nat Commun 2014;5:4233.
18) Ganley IG, Wong PM, Gammoh N, Jiang X. Distinct autophagosomal-lysosomal fusion mechanism revealed by thapsigargin-induced autophagy arrest. Mol Cell 2011;42:731-743.
19) Mauvezin C, Neufeld TP. Bafilomycin A1 disrupts autophagic flux by inhibiting both V-ATPase-dependent acidification and Ca-P60A/SERCA-dependent autophagosome-lysosome fusion. Autophagy 2015;11:1437-1438.
20) Park HW, Lee JH. Calcium channel blockers as potential therapeutics for obesity-associated autophagy defects and fatty liver pathologies. Autophagy 2014;10:2385-2386.
21) Matsumoto G, Wada K, Okuno M, Kurosawa M, Nukina N. Serine 403 phosphorylation of p62/SQSTM1 regulates selective autophagic clearance of ubiquitinated proteins. Mol Cell 2011;44:279-289.
22) Pilli M, Arko-Mensah J, Ponpuak M, Roberts E, Master S, Mandell MA, et al. TBK-1 promotes autophagy-mediated antimicrobial defense by controlling autophagosome maturation. Immunity 2012;37:223-234.
23) Clark K, Plater L, Peggie M, Cohen P. Use of the pharmacological inhibitor BX795 to study the regulation and physiological roles of TBK1 and IkappaB kinase epsilon: a distinct upstream kinase mediates Ser-172 phosphorylation and activation. J Biol Chem 2009;284:14136-14146.
24) **Reilly SM**, **Chiang SH**, Decker SJ, Chang L, Uhm M, Larsen MJ, et al. An inhibitor of the protein kinases TBK1 and IKK-epsilon improves obesity-related metabolic dysfunctions in mice. Nat Med 2013;19:313-321.
25) Barber GN. STING-dependent cytosolic DNA sensing pathways. Trends Immunol 2014;35:88-93.
26) Fu S, Watkins SM, Hotamisligil GS. The role of endoplasmic reticulum in hepatic lipid homeostasis and stress signaling. Cell Metab 2012;15:623-634.
27) Mukai K, Konno H, Akiba T, Uemura T, Waguri S, Kobayashi T, et al. Activation of STING requires palmitoylation at the Golgi. Nat Commun 2016;7:11932.
28) Cai X, Chiu YH, Chen ZJ. The cGAS-cGAMP-STING pathway of cytosolic DNA sensing and signaling. Mol Cell 2014;54:289-296.
29) West AP, Khoury-Hanold W, Staron M, Tal MC, Pineda CM, Lang SM, et al. Mitochondrial DNA stress primes the antiviral innate immune response. Nature 2015;520:553-557.
30) Rongvaux A, Jackson R, Harman CC, Li T, West AP, de Zoete MR, et al. Apoptotic caspases prevent the induction of type I interferons by mitochondrial DNA. Cell 2014;159:1563-1577.
31) Garcia-Martinez I, Santoro N, Chen Y, Hoque R, Ouyang X, Caprio S, et al. Hepatocyte mitochondrial DNA drives nonalcoholic steatohepatitis by activation of TLR9. J Clin Invest 2016;126:859-864.
32) Rolo AP, Teodoro JS, Palmeira CM. Role of oxidative stress in the pathogenesis of nonalcoholic steatohepatitis. Free Radic Biol Med 2012;52:59-69.
33) Katsuragi Y, Ichimura Y, Komatsu M. Regulation of the Keap1-Nrf2 pathway by p62/SQSTM1. Curr Opin Toxicol 2016;1:54-61.
34) Reilly SM, Ahmadian M, Zamarron BF, Chang L, Uhm M, Poirier B, et al. A subcutaneous adipose tissue-liver signalling axis controls hepatic gluconeogenesis. Nat Commun 2015;6:6047.
35) Friedman SL. Mechanisms of hepatic fibrogenesis. Gastroenterology 2008;134:1655-1669.
36) Parola M, Robino G. Oxidative stress-related molecules and liver fibrosis. J Hepatol 2001;35:297-306.
37) Komatsu M, Waguri S, Koike M, Sou YS, Ueno T, Hara T, et al. Homeostatic levels of p62 control cytoplasmic inclusion body formation in autophagy-deficient mice. Cell 2007;131:1149-1163.
38) Yu T, Yi YS, Yang Y, Oh J, Jeong D, Cho JY. The pivotal role of TBK1 in inflammatory responses mediated by macrophages. Mediators Inflamm 2012;2012:979105.
39) Aigelsreiter A, Neumann J, Pichler M, Halasz J, Zatloukal K, Berghold A, et al. Hepatocellular carcinomas with intracellular hyaline bodies have a poor prognosis. Liver Int 2017;37:600-610.
40) Bao L, Chandra PK, Moroz K, Zhang X, Thung SN, Wu T, Dash S. Impaired autophagy response in human hepatocellular carcinoma. Exp Mol Pathol 2014;96:149-154.
41) **Duran A**, **Hernandez ED**, **Reina-Campos M**, Castilla EA, Subramaniam S, Raghunandan S, et al. p62/SQSTM1 by Binding to Vitamin D Receptor Inhibits Hepatic Stellate Cell Activity, Fibrosis, and Liver Cancer. Cancer Cell 2016;30:595-609.
42) Oral EA, Reilly SM, Gomez AV, Meral R, Butz L, Ajluni N, et al. Inhibition of IKKvarepsilon and TBK1 Improves Glucose Control in a Subset of Patients with Type 2 Diabetes. Cell Metab 2017;26:157-170.e7.

Author names in bold designate shared co-first authorship.

Supporting Information

Additional Supporting Information may be found at onlinelibrary.wiley.com/doi/10.1002/hep.29742/suppinfo.